Jurnal Teknologi

Full paper

# Magnetic Induction Tomography: A Brief Review

Muhammad Saiful Badri Mansor[a], Zulkarnay Zakaria[b], Ibrahim Balkhis[b], Ruzairi Abdul Rahim[a*], Mohd Fadzli Abdul Sahib[c], Yusri Md. Yunos[a], Shafishuhaza Sahlan[a], Salinda Bunyamin[a], Khairul Hamimah Abas[a], Mohd Hafis Izran Ishak[a], Kumeresan A. Danapalasingam[a]

[a]*Process Tomography & Instrumentation Research Group (Protom-i), Infocomm Research Alliance, Control and Mechatronic Engineering Department, Universiti Teknologi Malaysia, 81310 UTM Johor Bahru, Johor, Malaysia*
[b]*Biomedical Electronic Engineering Department, School of Mechatronic Engineering, Universiti Malaysia Perlis, 02600 Arau, Perlis, Malaysia*
[c]*Faculty of Electrical and Electronic Engineering, Universiti Tun Hussein Onn Malaysia, 86400 Parit Raja, Batu Pahat, Johor, Malaysia*

*Corresponding author: ruzairi@fke.utm.my

**Article history**

Received :15 August 2014
Received in revised form :
5 January 2015
Accepted :10 February 2015

**Graphical abstract**

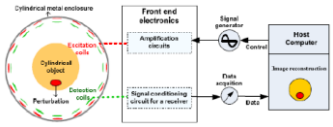

**Abstract**

Magnetic Induction Tomography (MIT) is a contactless non-invasive imaging technique that interested in mapping the passive electrical properties of a material; conductivity, permittivity and permeability. This paper presents the criteria and previous functional specification involving the development of MIT, focusing in conductivity imaging. Various ways have been implemented from a simple electronic configuration of the front-end sensory circuit, data acquisition system, reconstruction algorithm and graphical user interfacing (GUI) tools. Induction sensors are paramount as it does provide the signal source for time varying magnetic field to the coils. The advantages and limitations of MIT are also presented. Many more advancement can be expected to enhance the lack of MIT especially in spatial resolution and dynamic response of the sensor.

*Keywords*: Magnetic induction; conductivity; coils, algorithm



## 1.0 INTRODUCTION

MIT is an imaging technique used to image the electromagnetic properties of an object by using the eddy current effect [1]. It is also known as electromagnetic induction tomography, electromagnetic tomography (EMT), eddy current tomography, and eddy current testing. The method is used in non-destructive testing and geophysics, and has potential applications in process industry as well as in medicine. It is also used to generate 3D images of passive electrical properties (PEP), which has applications in brain imaging, cryosurgery monitoring in medical imaging, and metal flow visualization in metal working processes. Figure 1 shows the MIT block diagram developed by researchers from Glamorgan University.

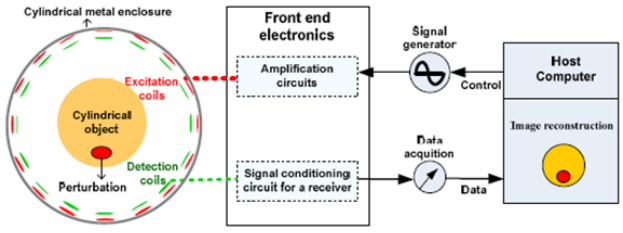


**Figure 1** glamorgan university mit system [25]

MIT applies a magnetic field from an excitation coil to induce eddy currents in the material. Thus the excitation magnetic field distribution is changed by the eddy currents, and the magnetic field resulting from these is then detected by sensing coils [2]. Figure 2 shows the resulting eddy current from conducting object under investigation. In medical applications, the eddy current field will change when the tissues' conductivity is changed by the disease. Consequently the measurement signal will also change and the tissues' pathology can be reflected by analysing this signal [3].

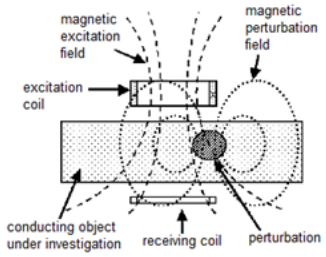


**Figure 2** The principle of magnetic induction tomography [25]

The principle of induction of eddy currents from an excited coil in MIT can be represented by a vector diagram, as shown in Figure 3. When biological tissue is exposed to the excitation magnetic field, ***B***, the tissue generates an eddy current due to the electromagnetic induction. The eddy current will also induce perturbation of the magnetic field, ΔB, which will change the strength and spatial distribution of the original excitation magnetic field. ΔB+B can be detected using the detection coils [4].

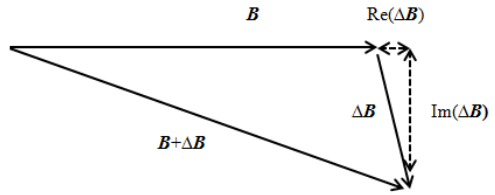


**Figure 3** Vector representation of the excitation magnetic field, *B*, and the perturbation magnetic field, ΔB [4]

This relationship undergoes mathematical derivation represented by Equation 1.

$$\Delta B/B \propto \omega(\omega\varepsilon_o\varepsilon_r - j\sigma) \quad (1)$$

where, ω is the angular frequency of the excitation coil, $\varepsilon_o$ is the vacuum permittivity, $\varepsilon_r$ is its relative permittivity, $j = \sqrt{-1}$ and σ is the conductivity of the tissue. The derivation shows that the total detected field ΔB + B lags the primary field B by an angle φ. The perturbation magnetic field ΔB contains a real part and an imaginary part. The real part of ΔB is caused by the displacement currents, and represents a linear relationship with the permittivity of the conductor. The imaginary part is caused by impedance. It is demonstrated that the phase-sensitive detection was necessary in order to obtain the distribution of tissue conductivity, which can be used to reconstruct the image [4].

## ■2.0 MAGNETIC PROPERTIES

A magnetic field has several properties: magnetic flux density; magnetic field intensity; total flux and magnetisation. These properties are briefly described in the following subchapter.

### 2.1 Magnetic Flux Density

Magnetic flux density in MIT is known as magnetic induction and, in free space, is theoretically defined as:

$$B = \mu_o H \quad (2)$$

where *B* is measured in Webers per square meter ($Wb/m^2$), or in a newer unit adopted in the International System of Units, the Tesla (T). An older unit that is often used for magnetic flux density is the Gauss (G), where 1 T or 1 $Wb/m^2$ is equal to 10,000 G. The constant $\mu_o$, the permeability in free space, is not dimensionless and has a defined value, in Henrys per meter (H/m), of:

$$\mu_o = 4\pi \times 10^{-7} H/m \quad (3)$$

The relative permeability of free space is important because the different materials exhibit their relative permeability. The magnetic field generated by the excitation coil can be calculated using the below equation:

$$B = \frac{\mu_o NI}{\sqrt{4R^2+L^2}} \quad (4)$$

### 2.2 Magnetic Field Intensity

The magnetic field intensity can be described, by using Ampere's circuital law: the line integral of *H* about any closed path is exactly equal to the direct current enclosed by that path. It is represented by Equation 5. The law is derived from the Biot-Savart law.

$$\oint H \cdot dl = I \quad (5)$$

where *H* is the magnetic field strength, which is produced by current *I*, and *dl* is a differential element of length along the path of integration. In SI units, *I* can be measured in Amperes (A) and *H* is measured in ampere-turns per meter (A/m). The field carries important information about the strength of the resultant field.

### 2.3 Total Flux

The total flux is the flux density applied over an area. Flux has the unit of a Weber, which is simply one Tesla[2].

### 2.4 Magnetization

Magnetisation is a measure of the extent to which an object is magnetised. It is a measure of the magnetic dipole moment per unit volume of the object. Magnetisation carries the same units as a magnetic field: amperes/meter.

## ■3.0 PASSIVE ELECTRICAL PROPERTIES

MIT has been widely applied to map an object under investigation based on three passive electrical properties of materials: conductivity (σ); permeability (μ) and permittivity (ε) [4-6]. Passive electrical properties are also known as dielectric properties. From the literature, it has been observed that in the researched material, much more focus is on the electrical conductivity profile, due to its relatively higher value compared to the other parameters.

Conductivity is the ability of materials to conduct an electrical current. In biological tissue, conductivity originates from the interaction of an electromagnetic wave with its environment at the cellular and molecular level [7, 34]. But the major difficulty in biomedical MIT that still remain, is the order of magnitude of the conductivity of biological tissues much more lower than metallic object. So the secondary field to be measured is relatively very weak [4].

In addition, a different phenomenon occurs when measuring the conductivity of metal for the process industry using MIT. Almost all metals show high electrical conductivity and these criteria allow MIT to distinguish metallic objects in the process industry. For example, [8] have developed a MIT system operating at higher frequency of 100 kHz to separate metallic objects (high conductivity, low permeability) from ferrite objects (low conductivity, high permeability) by the sign difference of the signal.

In early stage of the system development, measurements involving PEP require a physical connection to the patients via electrodes in order to inject weak AC currents and to measure the potential differences across sensing electrodes [9]. The diagnostic

information is extracted from the corresponding trans-impedances of the segment under investigation, also known as bio-impedance methods [9]. Measurements with a certain spatial resolution can be obtained using multichannel methods, for example when using EIT [9].

However the facts state that all bio-impedance electrode-based methods suffer from various drawbacks, such as the introduction of measurement errors due to the poorly defined electrode–skin interface, and the accuracy of absolute or static image reconstruction methods for EIT depends critically on the exact knowledge of the electrode locations. This requirement is difficult to fulfil because of the variability of the body surface geometry [9]. The intracranial applications are also difficult to perform in adults due to the high resistivity of the skull. Therefore EIT is less suitable to be used as an imaging tool when the subjects or samples have PEP characteristics.

## ■4.0 COILS AS INDUCTION SENSORS

Coils are one of the oldest, most well-known types of the magnetic sensor, and are also known as search coil sensors, pickup sensors and magnetic antennae [10, 35]. Coil sensors are only sensitive to the flux that is perpendicular to their main axis. Previous studies explained the operation of various types of induction sensors, such as *Rogowski* coils, gradiometer sensors, vibrating coil sensors, tangential field sensors and needle probes [10]. Fundamentally, there are two main designs of coil sensor, air core and ferromagnetic core. The low sensitivity of the air coil sensor can be partially overcome by the incorporation of a ferromagnetic core, which acts as a flux concentrator inside the coil. Figure 4 shows a typical *Rogowski* coil and air-core coil sensor.

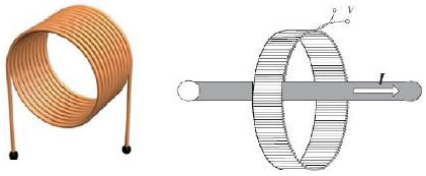

**Figure 4**: Air-core coil sensor and typical *Rogowski* coil for current measurement [10]

A ferrite core which has high permeability relative to the surrounding air is located at the centre of the screen and is capable of concentrating the primary magnetic field lines in the core material itself. The presence of the ferrite core, which made this design different from others, could increase the magnetic field of a coil by a factor of several thousand compared to use without the core [6].

An excitation coil can be designed in such a way as to help minimise the effect of the primary field [11-12]. Others have also proposed an exciting coil design, as shown in Figure 5, which has a conducting shield to protect the primary field from scatter around and to the outside [13]. Several techniques introduced by many researchers minimise the effect of the primary field at the peripheral end of the receiving coil in MIT. Among these techniques are:

1. Simple excitation and receiver coil with back-off coil.
2. Planar array that consists of an array of inductors on a printed circuit board [14].
3. Axial gradiometer with excitation coil sandwich in the differential coil [15].
4. Planar gradiometer (PGRAD)-differential coil printed on circuit board [16].
5. Zero flow coil (ZFC)-receiver coils with their axis perpendicular to the primary coil [17].
6. Zero flow planar gradiometer (ZFPGRAD)-planar gradiometer with its axis perpendicular to the primary coil [17].

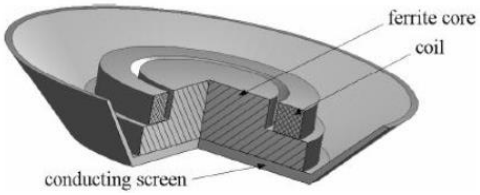


**Figure 5**: Exciting coil design with conducting shield [13].

## ■5.0 PREVIOUS CONDUCTIVITY MEASUREMENTS

Liu *et al.* have constructed an experiment to image a physical phantom using MIT [18]. The data acquisition system of MIT was formed of one exciting coil and 15 measuring coils. By rotating the conductivity perturbation of objects that placed on a circular plate, 16×15 measurement data points were obtained. The Newton-Raphson algorithm and the eigenvalue threshold regularisation method were applied to reconstruct the difference conductivity distribution images. The reconstructed images demonstrated the size and location of the objects, and identified a conductivity difference between 0.84 S/m and 1.26 S/m [18-19].

For high conductivity measurements, Ref. [20] has developed a novel planar EMT system for the detection of conductivity inhomogeneity in a metallic plate. The proposed system comprises six cylindrical coils that are distributed to form a circular array with all axes perpendicular to the plate under inspection. The sensitivity analysis of the system was carried out based on the numerical forward analytical solution technique, obtaining the Jacobian matrix. They applied some modifications to the Newton-Raphson method to measure the conductivity profile of the thin metal inhomogeneity and the results show that the system is capable of detecting the shape, direction and location of the flaw.

A feasibility study was carried out using a 3D arrangement, which comprises a human brain model and an array of 16 excitation coils and 32 receiving coils. The human brain model consists of about 35,000 tetrahedral finite elements and considers the cerebrospinal fluid around the brain, the grey matter, the white matter and a spherical oedema. The inverse problem is solved by means of a single step algorithm with four regularisation methods and the results show the possibility for detection of pathological hydration changes with good localisation [19].

The experiment carried out by [21] used a different approach to reconstruct the MIT conductivity image based on finite element method. Magnetically coupled conductivity sensors, [21] specifically when applied at multiple frequencies [9], appear attractive for monitoring pathologies in the brain that are correlated with local fluid shifts, *e.g.*, oedema, haemorrhages or epileptic events. The magnetic field penetrates easily through the skull and, due to the increased fluid accumulation; an oedema is represented by a greater or lesser localised perturbation of the conductivity within a normal brain.

Hamsch [22], through Philip's research group, began the development of a 16 channel MIT system with parallel readout receiver coil arrays using down-conversion techniques, which is quite similar to the classic annular array MIT architecture. The system operating frequency is 10 MHz. The direct digital synthesiser (DDS) has been chosen as the signal source and a new simultaneous 12 channel MOTU HD 24-bit 196 kHz analog-to-digital-converter (ADC) used to perform the process signal down-conversion. This technique provides a replacement for the commonly used lock-in amplifier and enables processing of all 16 receiving channels in parallel.

## 6.0 RECENT DEVELOPMENTS IN MAGNETIC INDUCTION TOMOGRAPHY

MIT has been exploited in many industrial and medical applications in various experimental setups, electronic measurement designs, enhancements of the reconstruction algorithm from either hybridisation and so on. Since its introduction and development during the last two decades, more detailed and advanced research into MIT has been explored and developed by many researchers worldwide. The development and recent achievements are described briefly in this subchapter.

In 2010, a novel MIT Direct Digitising Signal Measurement (DDSM) module has been developed for the classification of cerebral stroke a phase sensitive detection by [23]. The measurements are carried out using National Instrument (NI) PXI system. The highly technical system predefined 10MHz sine wave output, has been fed to a resistive divider, and followed by a set of differential amplifiers before the ADC. The gain between the input of the amplifier and the ADC was 3.6. The results show that the low phase noise of the presented system during the phase drifts measurements can be improved through the optimization of the amplifier design.

In 2011, a highly phase stable differential detector amplifier for biomedical MIT was developed by a group of researchers at the University of Glamorgan [24]. An array of gradiometry coil sensors was employed to reduce the detector coils' sensitivity to the primary reducing phase stability requirements [25-26]. The use of phase-stable amplifiers and the gradiometers' coil orientation need not be mutually exclusive, and it was reported that the highest measurement precision could be achieved by utilizing both approaches.

Following this, ref. [27] from the University of Bath developed a MIT system that focuses on industrial processing applications. The system used a NI-USB DAQ based system (NI-USB-6259) that is capable of generating sinusoidal signals and sensing the detected signals from the coil sensor simultaneously. The experiments were carried out for two coil sensor conditions, small scale and large scale. In the small scale experiments, the sensor array consisted of eight ferrite core coil inductors, which were experimentally proved to have capabilities for transmitting/detecting inductive signals independently. In the large scale experiments, the sensor array was expanded to make it more applicable for industrial applications, and consisted of eight air-core coils. The authors considered using the Tikhonov regularisation method linear algorithm because of its simplicity and the lower computational cost required. The results show that it is possible to image simple high conductivity structures.

Further developments in biomedical MIT in 2012 continued with the possibility of using a single rotating Tx–Rx coil, reported by [5]. It was agreed that by increasing the number of transmitters and receivers, a better image quality can be provided, but this will be at the expense of a larger and more expensive MIT system. Hence the rotational MIT system was proposed. In this system, the transceiver RF coil consisted of a three-turn surface coil loop with size about a quarter of the circumference placed inside the rotating acrylic cylinder. The coil was made of adhesive copper tape that was firmly adhered to the outside of the rotating cylinder. The digital control unit was implemented by using an Altera Cyclone III 3C120 digital signal processing (DSP) field programmable gate array (FPGA) development board. The result shows that the magnetic field profile of the rotational MIT coil provides a good field penetration depth towards the centre of the imaging area compared with conventional designs.

## 7.0 ADVANTAGES AND LIMITATIONS

MIT offers several advantages over the other types of tomographic modalities. The most well-known advantage of MIT is that MIT does not require direct contact with the samples, objects or materials to be examined. This has been beneficial in medical imaging where the attachment of many planes of electrodes, especially when conducting three-dimensional imaging, is inconvenient [28]. In addition, MIT with a large number of coil sensors could be built into the array and this could bring forward a solution for easy application to the patient [4].

MIT is also sensitive to the permeability of the material. Hence, it causes MIT highly applicable for industrial usage [8]. In magnetometer detection systems, a ferromagnetic tracer has been used in a solid meal to observe gastrointestinal movement, reported by [29]. Even though this is not an imaging modality and not yet tried in biomedical MIT, the technique exploits the contrast enhancement features of this field.

The next advantage of MIT is observed when the material to be imaged is entirely metallic and hence a very high conductivity [30]. In EIT, the trans-impedances would be very small indeed and difficult to be measured.

MIT also suffers from certain measurement difficulties and limitations. Firstly, it consists a capacitive coupling between an excitation coil and a receiving coil, which contaminates the measured value at the receiver. It is important to eliminate capacitive coupling so that the resultant measurement of eddy current signals represent the actual magnetically induced value [4]. These errors can be reduced using physical magnetic screening, differential amplification or by phase-sensitive detection.

The secondary signal in MIT is the one which carries information about the conductivity profile of the object being examined. It gradually weakens and easily superimposed by the primary signal from the transmitter. To eliminate the effect of the primary field on the secondary field, the subtraction method must be applied, which improves the sensitivity of the measurement. It can be achieved by using a separate sensing coil but this method is unlikely to be practical in a multipolar MIT system [31]. Ref. [32] describes a method of overlapping the excitation and sensing coils to reduce the primary signal, but this is only effective for the sensing coils immediately adjacent to the excitation coil.

It has led to the method of coil orientation at the transmitter as a solution for primary field cancelation at the receiving coil. The approach introduced by [33], that using a planar gradiometer as the sensor, enables most of the primary field to be cancelled in the sensor itself. By utilising the planar gradiometer orientation, the sensor can be made mechanically stable and thus exhibits a good primary field cancellation factor, but it does suffer from a few drawbacks. For multiple excitation coils, the primary signal is only cancelled out for one excitation coil position. Due to this limitation, [34] suggested an array of gradiometers adjusted for a single excitation coil, and rotation of the complete array to obtain the necessary set of projections [4].

## 8.0 CONCLUSION

Undoubtedly MIT is an ideal tomographic modality to be applied in both industrial process and biomedical tomography; foreign particle detection in food manufacturing, NDE testing, multiphase flow, lung and brain imaging, cancerous cell detection and so forth. It is believed that, by focusing the development of the algorithm, it can be the best approach to integrate with MIT inverse problems. Also, previous experimental works have been exposed with several ways to be adopted with vast different reconstruction algorithm. But, the target and focus to overcome the poorness in providing good resolution of the images is still under investigation.

## Acknowledgement

The author would like to thank Universiti Teknologi Malaysia for supporting the research study (vot. no. 03H96), MOE for FRGS grant (4F254) and also this appreciation goes to the other members in PROTOM-*i* research groups for their honorable cooperation.

## References

[1] Wei, H.Y., and Soleimani, M. 2012a. A Magnetic Induction Tomography System for Prospective Industrial Processing Applications. *Chinese Journal of Chemical Engineering.* 20: 406–410.

[2] Ziolkowski, M. and Gratkowski, S. 2009. Weighted Sum Method and Genetic Algorithm Based Multiobjective Optimization of an Exciter for Magnetic Induction Tomography. *Theoretical Engineering (ISTET), 2009 XV International Symposium on*. 1–5.

[3] Zinan, L., Zheng, X., and Haijun, L. 2008. The Application of Magnetic Sensor in MIT. *Automation Congress, WAC2008 World, VDE VERLAG Conference Proceedings*. 1–4.

[4] Griffiths, H. 2001. Magnetic Induction Tomography. *Measurement Science and Technology*. 12: 1126.

[5] Trakic, A., Eskandarnia, N., Li, B. K., Weber, E., Wang, H., Crozier, S. 2012. Rotational Magnetic Induction Tomography. *Measurement Science and Technology*. 23: 025402.

[6] Zakaria, Z., Rahim, R. A., Mansor, M. S. B., Yaacob, S., Ayub, N. M. N., Muji, S. Z. M., Rahiman, M. H. F., and Aman, S. M. K. S. 2012. Advancements in Transmitters and Sensors for Biological Tissue Imaging in Magnetic Induction Tomography. *Sensors*. 12: 7126–7156.

[7] Gabriel, C., Gabriel, S. and Corthout, E. 1996. The Dielectric Properties of Biological Tissues: I. Literature Survey. *Physics in Medicine and Biology*. 41: 2231.

[8] Peyton, A. J., Yu, Z. Z., Lyon, G., Al-Zeibak, S., Ferreira, J., Velez, J., Linhares, F., Borges, A. R., Xiong, H. L., Saunders, N. H. and Beck, M. S. 1996. An Overview of Electromagnetic Inductance Tomography: Description of Three Different Systems. *Measurement Science and Technology*. 7: 261.

[9] Scharfetter, H., Casanas, R. and Rosell, J. 2003. Biological Tissue Characterization by Magnetic Induction Spectroscopy (MIS): Requirements and Limitations. *Biomedical Engineering, IEEE Transactions on.* 50: 870–880.

[10] Tumanski, S. 2007. Induction Coil Sensors—A Review. *Measurement Science and Technology*. 18: R31.

[11] Soleimani, M., and Tamburrino, A. 2006. Shape Reconstruction in Magnetic Induction Tomography Using Multifrequency Data. *Int. J. Inf. Syst. Sci.* 2: 343–353.

[12] Yu, Z. Z., Peyton, A. J., Xu, L. A., and Beck, M. S. 1998. Electromagnetic Inductance Tomography (EMT): Sensor, Electronics and Image Reconstruction for A System With A Rotatable Parallel Excitation. *IEE Proceed. Sci. Meas. Technol.* 145: 20–25.

[13] Stawicki, K., Gratkowski, S., Komorowski, M., and Pietrusewicz, T. 2009. A New Transducer for Magnetic Induction Tomography. *IEEE Trans. Magn.* 45: 1832–1835.

[14] Gatzen, H. H., Andreeva, E., and Iswahjudi, H. 2002. Eddy-current Microsensors Based on Thin-Film Technology. *IEEE Trans. Magn.* 38: 3368–3370.

[15] Riedel, C. H., Keppelen, M., Nani, S., Merges, R. D. and Dossel, O. 2004. Planar System for Magnetic Induction Conductivity Measurement using a Sensor Matrix. *Physiol Meas.* 25(1): 403–11.

[16] Scharfetter, H., Merwa, R. and Pilz, K. 2004. *A New Type of Gradiometer for the Receiving Circuit of Magnetic Induction Tomography (MIT).* Translated by.

[17] Scharfetter, H., Merwa, R., and Pilz, K. 2005. A New Type of Gradiometer for the Receiving Circuit of Magnetic Induction Tomography (MIT). *Physiol Meas.* 26(2): S307–18.

[18] Liu, R., Li, Y., You, F., Shi, X., Fu, F., and Dong, X. 2008. Preliminary Imaging Results of Magnetic Induction Tomography Based on Physical Phantom, *Engineering in Medicine and Biology Society. 30th Annual International IEEE EMBS Conference*. 4559–4562.

[19] Liu, G., Wang, T., and Meng, M. 2005. A Fast Reconstruction Method for Magnetic Induction Tomography. *IEEE Proceedings of Engineering in Medicine and Biology*. 1663–1664.

[20] Yin, W. and Peyton, A. J. 2006. A Planar EMT System for The Detection of Faults On Thin Metallic Plates. *Measurement Science and Technology.* 17: 2130.

[21] Merwa, R., and Scharfetter, H. 2007. Magnetic Induction Tomography: A Feasibility Study of Brain Oedema Detection using a Finite Element Human Head Model. *IFMBE Proceedings.* 17: 480–483.

[22] Hamsch, M., Igney, C. H. and Vauhkonen, M. 2007. *16 Channel Magnetic Induction Tomography System Featuring Parallel Readout*. Translated by Graz, Austria.

[23] Patz, R., Watson, S., Ktistis, C., Hamsch, M. and Peyton, A. J. 2010. Performance of a FPGA-based Direct Digitising Signal Measurement module for MIT. *Journal of Physics: Conference Series.* 224: 1–4.

[24] Watson, S., Wee, H. C., Griffiths, H., and Williams, R. J. 2011. A Highly Phase-Stable Differential Detector Amplifier for Magnetic Induction Tomography. *Physiological Measurement.* 32: 917.

[25] Igney, C. H., Watson, S., Williamson, S. J., Griffiths, H. and Dössel, O. 2005. Design and Performance of A Planar-Array MIT System With Normal Sensor Alignment. *Physiological Measurement.* 26(2): S263–S278.

[26] Scharfetter, H., Kostinger, A., and Issa, S. 2008. Hardware for Quasi-Single-Shot Multifrequency Magnetic Induction Tomography (MIT): The Graz Mk2 System *Physiol. Meas.* 29: S431–43

[27] Wei, H. Y., and Soleimani, M. 2012. Hardware and Software Design for a National Instrument-Based Magnetic Induction Tomography System for Prospective Biomedical Applications. *Physiological Measurement.* 33: 863.

[28] Metherall, P., Barber, D. C., Smallwood, R. H., and Brown, B. H. 1996. Three-Dimensional Electrical Impedance Tomography. *Nature.* 380: 509–12.

[29] Forsman, K. 2000. Intragastric Movement Assessment by Measuring Magnetic Field Decay of Magnetised Tracer Particles in a Solid Meal. *Med. Biol. Eng. Comput.* 38(2): 169–74.

[30] Pham. M., H., Hua, Y., and Gray, N., B. 1999. Eddy Current Tomography for Metal Solidification Imaging. *Proc. 1st World Congrss on Industrial Process Tomography, Buxton, UK, 14–17 April*. 451–8.

[31] Griffiths, H., Stewart, W., R., and Gough, W. 1999. Magnetic Induction Tomography: A Measuring System for Biological Tissues. *Ann. NY Acad. Sci.* 873: 335–45

[32] Peyton, A. J., Beck, M. S., Borges, A. R., Oliveira, J. E., Lyon, G. M., Yu, Z. Z., Brown, M. W., and Ferrerra, J. 1999. Development of Electromagnetic Tomography (EMT) for Industrial Applications. Part 1: Sensor Design and Instrumentation. *1st World Congress on Industrial Process Tomography, Buxton, Greater Manchester, April 14-17, 1999.* 306–312.

[33] Scharfetter, H., Lackner, H. K., and Rosell, J. 2001. Magnetic Induction Tomography: Hardware for Multifrequency Measurements in Biological Tissues *Physiol. Meas.* 25: 131–46.

[34] Rosell, J., Casanas, R., and Scharfetter, H. 2001. Sensitivity Maps and System Requirements for Magnetic Induction Tomography using A Planar Gradiometer *Physiol. Meas.* 22: 121–30.

[34] Z. Zakaria, M. F. Jumaah, M. S. B. Mansor, M. Mat Daud, M. H. Fazalul Rahiman, R. Abdul Rahim. January 2011. Initial Results On Medium Frequency Electromagnetic Field Penetration In Biological Soft Tissue. *Jurnal Teknologi-Special Issue on Instrumentation & Sensor Technology.* Universiti Teknologi Malaysia. 54: 69–77.

[35] N. M. Nor Ayob, Z. Zakaria, M. H. Hafiz Fazalul Rahiman, R. Abdul Rahim, S. Yaacob. August 2011. Initial Development On Magnetic Induction Tomography Imaging. *Jurnal Teknologi-Special Issue on Instrumentation & Sensor Technology.* Universiti Teknologi Malaysia. 55(2): 11–14.